2009

Scaling of Sweet–Parker reconnection with secondary islands

P. A. Cassak

M. A. Shay

J. F. Drake

Scaling of Sweet–Parker reconnection with secondary islands

P. A. Cassak,[1] M. A. Shay,[2] and J. F. Drake[3]
[1]*Department of Physics, West Virginia University, Morgantown, West Virginia 26506, USA*
[2]*Department of Physics and Astronomy, University of Delaware, Newark, Delaware 19716, USA*
[3]*Department of Physics and Institute for Research in Electronics and Applied Physics, University of Maryland, College Park, Maryland 20742, USA*

(Received 21 September 2009; accepted 23 November 2009; published online 9 December 2009)

Sweet–Parker (collisional) magnetic reconnection at high Lundquist number is modified by secondary islands. Daughton *et al.* [Phys. Rev. Lett. **103**, 065004 (2009)] suggested the Sweet–Parker model governs the fragmented current sheet segments. If true, the reconnection rate would increase by the square root of the number of secondary islands. High Lundquist number resistive magnetohydrodynamic simulations are presented which agree, in a time-averaged sense, with the predicted scaling. This result may have important implications for energy storage before a solar eruption and its subsequent release. © *2009 American Institute of Physics*.
[doi:10.1063/1.3274462]

The Sweet–Parker model of magnetic reconnection[1,2] predicts $E \sim S^{-1/2}$, where E is the (normalized) reconnection rate, $S = 4\pi c_A L_{SP}/\eta c^2$ is the Lundquist number, η is the resistivity, L_{SP} is the half length of the diffusion region, and c_A is the Alfvén speed based on the reconnecting magnetic field. This has been confirmed by laboratory experiments[3–5] and numerical simulations (e.g., Ref. 6) in the limit of small or modest $S < S_{crit}$, where $S_{crit} \sim 10^4$. However, for $S > S_{crit}$, secondary islands fragment the diffusion region.[6] Secondary islands, known as plasmoids upon ejection from the current sheet, are observed in many contexts (e.g., Refs. 7–9).

There is no accepted quantitative model of Sweet–Parker reconnection with secondary islands although it is surely faster than the classical model. The critical issue is *how much* faster. In this context, we define "fast" reconnection as having a rate independent of or weakly dependent on the dissipation mechanism and system size and being fast enough to explain observations, while "slow" reconnection has a rate depending strongly on the dissipation mechanism and system size. It has been suggested that secondary islands (whether due to secondary tearing or externally driven turbulence) make Sweet–Parker reconnection faster.[10–13] Elevated rates have been observed in many simulation studies,[14–18] but it remains unknown if the reconnection is fast or slow. A recent study[19] found the reconnection rate is weakly dependent on S for S up to 6.3×10^5.

Determining the rate of reconnection is critical for applications in the solar corona, where huge amounts of energy can lie dormant for hours before flares. Plasmas with free magnetic energy contain currents which invariably contain sites where reconnection is prone to occur. If reconnection is always fast because of secondary islands (or they cause a rapid transition to fast reconnection), then any reconnection event would release the stored energy so energy would have to be stored without any reconnection taking place. This is difficult to envision in the complicated magnetic topologies in active regions, so a new understanding of what prevents reconnection would be needed. If reconnection can be slow then it would not interfere with preflare energy storage. A different mechanism explaining fast reconnection would need to be invoked, such as collisionless effects.[20–27] (The role of secondary islands on the transition to collisionless reconnection is addressed in a companion paper.[28])

Recently, a quantitative model was suggested in which Sweet–Parker scaling describes each segment of the fragmented current sheet.[29] This implies E increases like the square root of the number of secondary islands N when $S > S_{crit}$. In this letter, we investigate the scaling of Sweet–Parker reconnection with N using high-S magnetohydrodynamic (MHD) simulations. Our results support Ref. 29 in a time-averaged sense during suitably quasisteady evolution of up to $S \simeq 10^5$. ("Quasisteady evolution" is defined later.) If the present result scales to coronal parameters, it provides a way to estimate the collisional reconnection rate for a given secondary island generation model. This determines whether the reconnection is fast or slow, which is important for coronal energy storage and release.

The theory of the effect of secondary islands[29] is relatively simple. A diffusion region of half length L_{SP} with N secondary islands is cut into pieces of length $L \sim L_{SP}/N$. If the Sweet–Parker model describes each segment, the thickness δ of the segments scales as

$$\delta \sim \frac{\delta_{SP}}{\sqrt{N}}, \tag{1}$$

where δ_{SP} is the thickness predicted by the classical Sweet–Parker theory.[2] Since $E \sim \delta/L$, one finds

$$E \sim E_{SP}\sqrt{N}, \tag{2}$$

where $E_{SP} \sim S^{-1/2}$ is the classical Sweet–Parker rate. We emphasize that these results apply for two-dimensional reconnection in the fully nonlinear regime once a quasisteady state has been reached with secondary islands continuously being generated and convected downstream.

Since $N > 1$, Eq. (2) implies secondary islands speed up Sweet–Parker reconnection. Physically, this arises because secondary islands contain more plasma than a laminar cur-

TABLE I. Parameters for the simulations ($L, S_g, S, \Delta, D_4, W_0, B_{\rm coh}, B_{\rm incoh}$) and time-averaged results ($E, \delta, N_{\rm cons}, N_{\rm lib}$).

$L(L_0)$	S_g	S	$\Delta(L_0)$	$D_4(10^{-5}c_{A0}L_0^3)$	$W_0(L_0)$	$B_{\rm coh}(10^{-3}B_0)$	$B_{\rm incoh}(10^{-5}B_0)$	$E(E_0)$	$\delta(L_0)$	$N_{\rm cons}$	$N_{\rm lib}$
102.4	3.4×10^4	8.5×10^3	0.05	0.375	0.2	0.75	0.125	0.0110	0.289	1.00	1.00
204.8	6.8×10^4	1.7×10^4	0.05	0.375	0.3	1.6875	0.281 25	0.0118	0.283	2.14	3.07
409.6	1.4×10^5	3.4×10^4	0.10	6.00	0.4	3.0	0.5	0.0106	0.352	3.06	4.41
819.2	2.7×10^5	6.8×10^4	0.10	6.00	0.6	6.0	1.0	0.0116	0.313	4.68	7.56

rent layer so the particle flux carried by these islands as they convect downstream helps alleviate the outflow bottleneck in the classical Sweet–Parker model.

To test these predictions, we employ two-dimensional compressible resistive-MHD simulations using the F3D code[30] in a periodic domain of size $L\times L/2$ with a grid scale Δ. Lengths, magnetic fields, and densities are normalized to arbitrary values L_0, B_0, and n_0, while velocities, times, electric fields, and resistivities are normalized to the Alfvén speed $c_{A0}=B_0/(4\pi m_i n_0)^{1/2}$, the Alfvén time L_0/c_{A0}, $E_0=c_{A0}B_0/c$, and $\eta_0=4\pi c_{A0}L_0/c^2$, respectively, where e and m_i are the ion charge and mass.

The resistivity is constant and uniform for all simulations with a value of $\eta=0.003$; the global Lundquist number is $S_g=L/\eta$. Ohmic heating is ignored and there is no viscosity. The temperature $T=1$ is uniform and not evolved. Fourth order diffusion in all equations damps noise at the grid scale with an amplitude D_4 giving the same damping rate for varying grid scale. The initial configuration is a double tearing mode, $B_x(y)=\tanh[(y-L/8)/W_0]-\tanh[(y-3L/8)/W_0]-1$, where W_0 is the initial current layer thickness. Total pressure is balanced initially using a nonuniform density. A single X-line is seeded using a coherent magnetic perturbation $B_{\rm coh}$. Initial random magnetic perturbations $B_{\rm incoh}$ break symmetry so secondary islands are ejected. There is no guide field.

In the present study, we vary the system size L with a fixed η. Table I shows the parameters used for the simulations. Convergence tests on D_4 have been carried out. For smaller systems, the diffusion region is narrower so higher resolution is necessary to ensure numerical dissipation at the grid scale does not play a role. For periodic simulations, $L_{\rm SP}\sim L/4$, so $S\sim S_g/4$ and ranges up to 6.8×10^4 (a factor of 3 smaller than the largest runs in Ref. 19). From the Biskamp criterion[6] of $S_{\rm crit}\sim10^4$, the smallest system is stable to secondary island formation, while the other three are unstable.

The (global) reconnection rate E is determined as the time rate of change in the difference in magnetic flux ψ between the main X- and O-lines (the extrema in ψ along the neutral line). The number of islands N equals the number of X-lines. This is determined by identifying candidates as locations where the reconnected field B_y changes sign along the neutral line. Visual inspection is used to count active X-lines. To allow for interpretational variability, we use counts of X-lines based on a conservative criterion $N_{\rm cons}$ (only those with robust observable X-line characteristics) and a liberal criterion $N_{\rm lib}$ (every possible candidate within the current sheet) and present the analysis using both.

The reconnection rate and number of X-lines are plotted as a function of time in Fig. 1 for each simulation, with E as the dashed black line using the axis labels on the left. The thin red lines give N using the labels on the right, with the solid (dashed) line as $N_{\rm cons}$ ($N_{\rm lib}$). Since E varies in time, the plotted values are smoothed (over half an Alfvén transit time or less) to emphasize the average properties.

The horizontal dotted-dashed line marks the classical Sweet–Parker prediction $E_{\rm SP}$ assuming $L_{\rm SP}=L/4$. For the smallest system, there is only a single X-line (following tran-

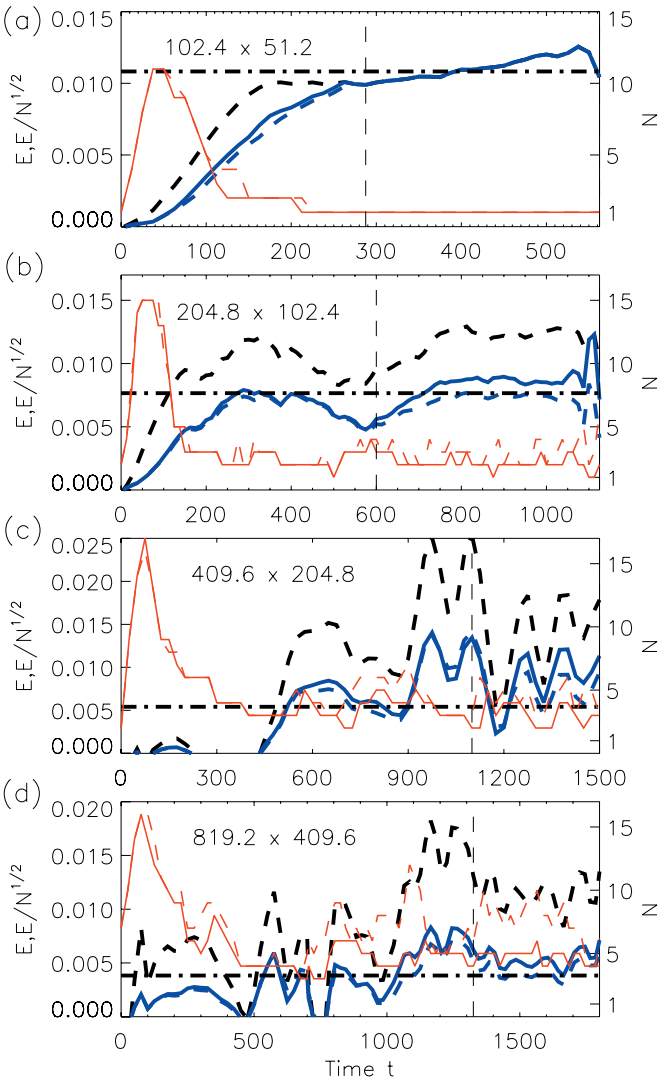

FIG. 1. (Color) Reconnection rate E (dashed black line) and number of X-lines N (thin red line) as a function of time for systems of increasing size. For N, the solid (dashed) line shows $N_{\rm cons}$ ($N_{\rm lib}$). The vertical dashed lines show where a quasisteady state begins. The thick blue lines show $E/N^{1/2}$ (solid using $N_{\rm cons}$, dashed using $N_{\rm lib}$). The horizontal dashed-dotted line shows the predicted $E_{\rm SP}$, revealing good agreement.

sients), and E agrees well with E_{SP}. For all other runs, the number of secondary islands remains larger than 1, in agreement with the Biskamp criterion, and E exceeds E_{SP}.

To make meaningful comparisons with the theory, we focus on quasisteady times during the nonlinear phase (we exclude the early transient phase during which a system size island forms). We define "quasisteady times" as having secondary islands continually being generated, convected down and out of the sheet, and regenerated. We observe that E and N vary during this time about a relatively steady value.

These assumptions do not always hold. For example, consider an island generated near the left edge of the sheet convecting to the right. If another island emerges further to the right, the first island can slow down or temporarily stop. During this time, E is observed to decrease. When the island moves again, E increases. This behavior is presumably relevant for physical systems, but have been eliminated from the analysis. This is discussed further in the conclusions.

The vertical dashed lines in Fig. 1 show when the steady evolution begins. The thick blue line shows $E/N^{1/2}$, with the solid (dashed) line using N_{cons} (N_{lib}). The $E/N^{1/2}$ values line up well with E_{SP}, in agreement with Eq. (2).

The thickness δ, measured as the e-folding distance across the sheet at the main X-line, is plotted in Fig. 2 as a function of time as the dashed black line. The blue lines show $N^{1/2}\delta$ using N_{cons} (solid) and N_{lib} (dashed). The horizontal line shows the predicted δ_{SP}, which agrees well with $N^{1/2}\delta$ as predicted by Eq. (1). Note that Fig. 2 reveals that the number of grid cells across the full current layer is between 6 and 12 for each run, confirming that the resolution is sufficient to keep grid scale dissipation small.

To address the scaling, averages over the steady times of E, δ, N_{cons}, and N_{lib} are in Table I. Raw values of E agree with recent simulations.[19] Figure 3 shows E and δ normalized to $N^{1/2}$ as a function of S, with diamonds (squares) denoting use of N_{cons} (N_{lib}). The data follow the expected Sweet–Parker scaling (dashed-dotted line). We conclude, for the systems in the present study, that Eqs. (1) and (2) appropriately describe the speed-up of Sweet–Parker reconnection due to secondary islands during quasisteady evolution (when the current sheet thickness exceeds kinetic scales[29,31]).

What do the present results imply about solar eruptions? Such a determination is premature. The model does not incorporate interactions between islands and there is no guarantee that the results scale to larger S. The results may not scale to large S due to a hierarchical progression of secondary island formation, whereby current sheets between secondary islands themselves generate secondary islands,[22,29] an effect which has been reported in simulations.[19]

Nonetheless, it is instructive to give results for coronal applications if the results do scale to large S. Suppose

$$N \sim (S/S_{crit})^{\alpha} \tag{3}$$

for some α, where $S_{crit} \sim 10^4$. Then, from Eq. (2), $E \propto S^{-(1-\alpha)/2}$. Specifying the island generation model (i.e., α) gives the reconnection rate.

The critical issue is how much faster the process becomes. If N approximately scales with S ($\alpha \sim 1$), then E is weakly dependent on system size and dissipation mechanism, and is fast. If $\alpha < 1$, then E depends strongly on S so reconnection is slow. This is because the classical Sweet–Parker rate is six orders of magnitude slower than observed energy release rates so a speed-up by even three orders of magnitude is slower than fast reconnection.

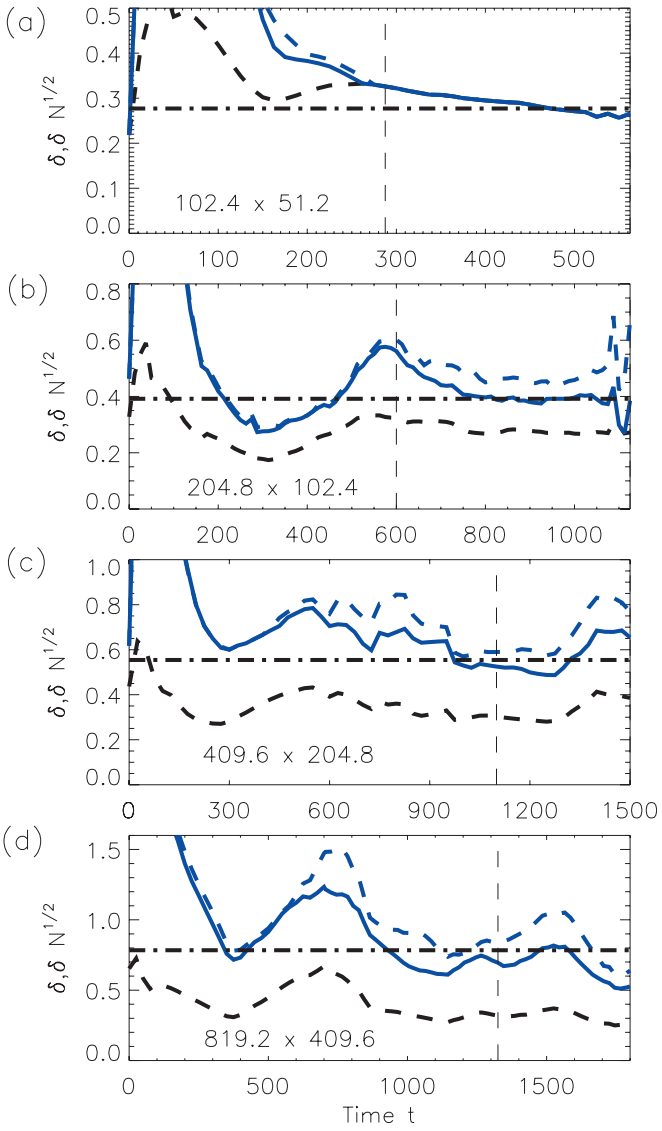

FIG. 2. (Color) Current sheet thickness δ (dashed black line) at the main X-line as a function of time for the simulations in Fig. 1. The thick blue lines show $N^{1/2}\delta$ (solid using N_{cons}, dashed using N_{lib}) and the horizontal dashed-dotted line shows the predicted δ_{SP}, revealing good agreement.

A recent study used linear theory to predict $\alpha = 3/8$,[32] later confirmed in MHD simulations.[33] However, there is no reason to expect linear theory holds for fully nonlinear systems under present consideration. Simulations of nonlinear reconnection are finding higher values; $\alpha \sim 0.6$ was reported in particle-in-cell simulations with $S \lesssim 4 \times 10^4$.[29] The present data yield $\alpha \sim 0.72$ using N_{cons} and $\alpha = 0.93$ using N_{lib}, although there are only three data points. Our results and similar results in Ref. 19 cannot rule out $\alpha \sim 1$ (see Table I) although future runs with $S \gg 10^5$ are required.

Another application is the chromosphere, where the Sweet–Parker model may be valid.[34–36] The reconnection rate is a few times larger than the classical Sweet–Parker

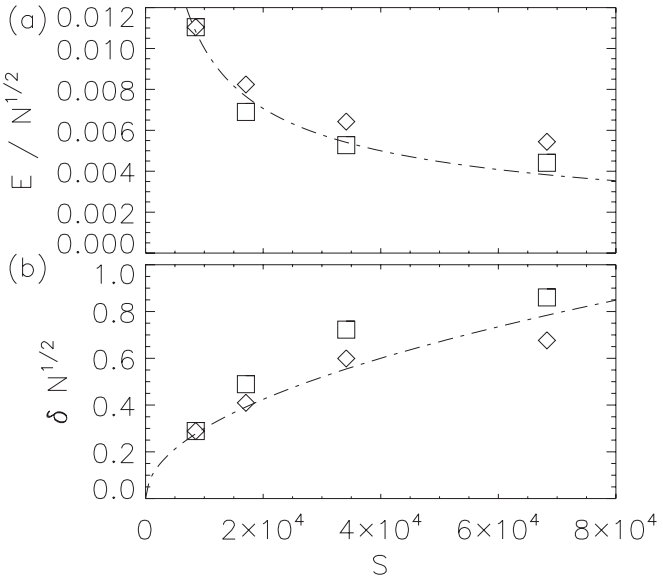

FIG. 3. (a) Reconnection rate E and (b) thickness δ, averaged over the steady time and normalized to $N^{1/2}$, as a function of Lundquist number S. The dashed line is the classical Sweet–Parker prediction. Diamonds (squares) use N_{cons} (N_{lib}).

prediction.[35] Using Eqs. (2) and (3), a speed-up by a factor of 5 for $S \sim 10^6 - 10^8$ occurs for $\alpha - 0.7 - 0.35$. Secondary islands may give closer agreement with the observations.

The present simulations contain limitations which should be addressed in future research. A constant resistivity is employed instead of a Spitzer resistivity.[29,31] Ohmic heating and viscosity are omitted, the latter of which may be important for secondary island generation.[37] Three-dimensional effects are potentially important. The simulations should be extended to higher S as resources allow. The simulations do not contain a guide field, expected to be present in the corona, which may or may not impact secondary islands.

In the present simulations, the identity of the main X-line is preserved through most of the evolution. X-line identity may be preserved in physical systems, but it is not required, so a more general technique for quantifying E is needed for such systems. The results do not apply to systems in which secondary islands are stationary in the current sheet. It is important to incorporate the full range of dynamics of islands into the model (see Ref. 38 for one approach). Finally, we emphasize that the present study concerns self-consistent generation of secondary islands, not the effect of externally imposed turbulence.[12,15,17,18]

The authors acknowledge helpful conversations with W. Daughton and A. A. Schekochihin. Computations used resources at the National Energy Research Scientific Computing Center. The authors gratefully acknowledge support by the NSF under Grant Nos. PHY-0902479 (P.A.C.), PHY-0316197 (J.F.D.), and ATM-0645271 (M.A.S.), and by NASA under Grant No. NNX08AM37G (M.A.S.).

[1] P. A. Sweet, in *Electromagnetic Phenomena in Cosmical Physics*, edited by B. Lehnert (Cambridge University Press, New York, 1958), p. 123.
[2] E. N. Parker, J. Geophys. Res. **62**, 509, doi:10.1029/JZ062i004p00509 (1957).
[3] H. Ji, M. Yamada, S. Hsu, and R. Kulsrud, Phys. Rev. Lett. **80**, 3256 (1998).
[4] F. Trintchouk, M. Yamada, H. Ji, R. M. Kulsrud, and T. A. Carter, Phys. Plasmas **10**, 319 (2003).
[5] I. Furno, T. P. Intrator, E. W. Hemsing, S. C. Hsu, S. Abbate, P. Ricci, and G. Lapenta, Phys. Plasmas **12**, 055702 (2005).
[6] D. Biskamp, Phys. Fluids **29**, 1520 (1986).
[7] K. K. Reeves, T. B. Guild, W. J. Hughes, K. E. Korreck, J. Lin, J. Raymond, S. Savage, N. A. Schwadron, H. E. Spence, D. F. Webb, and M. Wiltberger, J. Geophys. Res. **113**, A00B02, doi:10.1029/2008JA013049 (2008).
[8] J. Lin, S. R. Cranmer, and C. J. Farrugia, J. Geophys. Res. **113**, A11107, doi:10.1029/2008JA013409 (2008).
[9] M. G. Linton and M. B. Moldwin, J. Geophys. Res. **114**, A00B09, doi:10.1029/2008JA013660 (2009).
[10] W. H. Matthaeus and S. L. Lamkin, Phys. Fluids **29**, 2513 (1986).
[11] B. Kliem, in *Coronal Magnetic Energy Releases, Lecture Notes in Physics*, edited by A. O. Benz and A. Krüger (Springer, Berlin, 1995), Vol. 444, p. 93.
[12] A. Lazarian and E. Vishniac, Astrophys. J. **517**, 700 (1999).
[13] G. Lapenta, Phys. Rev. Lett. **100**, 235001 (2008).
[14] Q.-L. Fan, X.-S. Feng, and C.-Q. Xiang, Phys. Plasmas **11**, 5605 (2004).
[15] D. Smith, S. Ghosh, P. Dmitruk, and W. H. Matthaeus, Geophys. Res. Lett. **31**, L02805, doi:10.1029/2003GL018689 (2004).
[16] L. Ni, A. Bhattacharjee, and H. Yang, Bull. Am. Phys. Soc. **53**, 94 (2008).
[17] G. Kowal, A. Lazarian, E. T. Vishniac, and K. Otmianowska-Mazur, Astrophys. J. **700**, 63 (2009).
[18] N. F. Loureiro, D. A. Uzdensky, A. A. Schekochihin, S. C. Cowley, and T. A. Yousef, Mon. Not. R. Astron. Soc. **399**, L146 (2009).
[19] A. Bhattacharjee, Y.-M. Huang, H. Yang, and B. Rogers, Phys. Plasmas **16**, 112102 (2009).
[20] D. Biskamp, E. Schwarz, and J. F. Drake, Phys. Rev. Lett. **75**, 3850 (1995).
[21] Z. W. Ma and A. Bhattacharjee, Geophys. Res. Lett. **23**, 1673, doi:10.1029/96GL01600 (1996).
[22] K. Shibata and S. Tanuma, Earth, Planets Space **53**, 473 (2001).
[23] A. Bhattacharjee, Annu. Rev. Astron. Astrophys. **42**, 365 (2004).
[24] P. A. Cassak, M. A. Shay, and J. F. Drake, Phys. Rev. Lett. **95**, 235002 (2005).
[25] P. A. Cassak, J. F. Drake, and M. A. Shay, Astrophys. J. **644**, L145 (2006).
[26] D. A. Uzdensky, Astrophys. J. **671**, 2139 (2007).
[27] P. A. Cassak, D. J. Mullan, and M. A. Shay, Astrophys. J. Lett. **676**, L69 (2008).
[28] P. A. Cassak and J. F. Drake, Astrophys. J. Lett. **707**, L158 (2009).
[29] W. Daughton, V. Roytershteyn, B. J. Albright, H. Karimabadi, L. Yin, and K. J. Bowers, Phys. Rev. Lett. **103**, 065004 (2009).
[30] M. A. Shay, J. F. Drake, M. Swisdak, and B. N. Rogers, Phys. Plasmas **11**, 2199 (2004).
[31] W. Daughton, V. Roytershteyn, B. J. Albright, H. Karimabadi, L. Yin, and K. J. Bowers, Phys. Plasmas **16**, 072117 (2009).
[32] N. F. Loureiro, A. A. Schekochihin, and S. C. Cowley, Phys. Plasmas **14**, 100703 (2007).
[33] R. Samtaney, N. F. Loureiro, D. A. Uzdensky, A. A. Schekochihin, and S. C. Cowley, Phys. Rev. Lett. **103**, 105004 (2009).
[34] Y. E. Litvinenko, Astrophys. J. **515**, 435 (1999).
[35] J. Chae, Y.-J. Moon, and S.-Y. Park, J. Korean Astron. Soc. **36**, S13 (2003).
[36] Y. E. Litvinenko and J. Chae, Astron. Astrophys. **495**, 953 (2009).
[37] W. Park, D. A. Monticello, and R. B. White, Phys. Fluids **27**, 137 (1984).
[38] R. Fermo, J. F. Drake, and M. Swisdak, "A statistical model of magnetic islands in a current layer," Phys. Plasmas (submitted).